

# Human Neural Larva Migrans Caused by *Ophidascaris robertsi* Ascarid

Mehrab E Hossain, Karina J. Kennedy, Heather L. Wilson, David Spratt, Anson Koehler, Robin B. Gasser, Jan Šlapeta, Carolyn A. Hawkins, Hari Priya Bandi, Sanjaya N. Senanayake

We describe a case in Australia of human neural larva migrans caused by the ascarid *Ophidascaris robertsi*, for which Australian carpet pythons are definitive hosts. We made the diagnosis after a live nematode was removed from the brain of a 64-year-old woman who was immunosuppressed for a hypereosinophilic syndrome diagnosed 12 months earlier.

*Ophidascaris* species are nematodes exhibiting an indirect lifecycle; various genera of snakes across the Old and New Worlds are definitive hosts. *O. robertsi* nematodes are native to Australia, where the definitive hosts are carpet pythons (*Morelia spilota*). The adult nematodes inhabit the python's esophagus and stomach and shed their eggs in its feces. Eggs are ingested by various small mammals, in which larvae establish, serving as intermediate hosts (1). Larvae migrate to thoracic and abdominal organs (1–3) where, particularly in marsupials, the third-stage larvae may reach a considerable length (7–8 cm), even in small hosts (3,4). The lifecycle concludes when pythons consume the infected intermediate hosts (3). Humans infected with *O. robertsi* larvae would be considered accidental hosts, although human infection with any *Ophidascaris* species has not previously been reported. We report a case of human neural larva migrans caused by *O. robertsi* infection.

## The Study

A 64-year-old woman from southeastern New South Wales, Australia, was admitted to a local hospital in late January 2021 after 3 weeks of abdominal pain and diarrhea, followed by dry cough and night sweats. She had a peripheral blood eosinophil count (PBEC) of  $9.8 \times 10^9$  cells/L (reference range  $<0.5 \times 10^9$  cells/L), hemoglobin 99 g/L (reference range 115–165 g/L), platelets  $617 \times 10^9$  cells/L (reference range 150–400  $\times 10^9$  cells/L), and C-reactive protein (CRP) 102 mg/L (reference range  $<5$  mg/L). Her medical history included diabetes mellitus, hypothyroidism, and depression. She was born in England and had traveled to South Africa, Asia, and Europe 20–30 years earlier. She was treated for community-acquired pneumonia with doxycycline and had not recovered fully.

A computed tomography (CT) scan revealed multifocal pulmonary opacities with surrounding ground-glass changes, as well as hepatic and splenic lesions. Bronchoalveolar lavage revealed 30% eosinophils without evidence of malignancy or pathogenic microorganisms, including helminths. Serologic testing was negative for *Strongyloides*. Autoimmune disease screening results were negative. The patient's diagnosis was eosinophilic pneumonia of unclear etiology; she began taking prednisolone (25 mg/d) with partial symptomatic improvement.

Three weeks later, she was admitted to a tertiary hospital with recurrent fever and a persistent cough while on prednisolone. PBEC was  $3.4 \times 10^9$  cells/L and CRP was 68.2 mg/L. CT scans revealed persistent hepatic and splenic lesions and migratory pulmonary opacities (Figure 1, panels A, B). The pulmonary and hepatic lesions were 18F-fluorodeoxyglucose-avid on positive emission tomography scan. Lung biopsy specimen was consistent with eosinophilic pneumonia but not with eosinophilic granulomatosis with polyangiitis (EGPA) (Figure 1, panel C). Bacterial, fungal, and mycobacterial cultures were negative.

Author affiliations: Canberra Health Services, Canberra, Australian Capital Territory, Australia (M. Hossain, K.J. Kennedy, H.L. Wilson, C.A. Hawkins, H. Bandi, S.N. Senanayake); Australian National University, Canberra (K.J. Kennedy, C.A. Hawkins, H. Bandi, S.N. Senanayake); Commonwealth Scientific and Industrial Research Organization Australian Capital Territory, Canberra (D. Spratt); University of Melbourne, Melbourne, Victoria, Australia (A. Koehler, R.B. Gasser); University of Sydney, Sydney, New South Wales, Australia (J. Šlapeta); The University of Sydney Institute for Infectious Diseases, Sydney (J. Šlapeta)

DOI: <http://doi.org/10.3201/eid2909.230351>

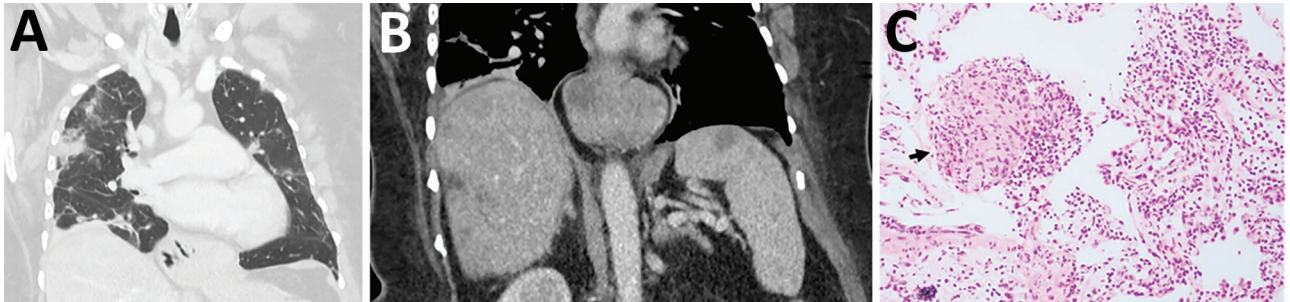


**Figure 1.** Early testing conducted during investigation of illness in a 64-year-old woman from southeastern New South Wales, Australia, who was later determined to have *Ophidascaris robertsi* nematode infection. A) Computed tomography scan of chest with venous contrast demonstrating multiple bilateral airspace opacities and nodules with a peripheral bronchovascular distribution. The opacities have surrounding ground-glass changes. Many were present in the patient's study from a previous hospitalization; however, some had resolved while others were new, indicating a migratory pattern. B) Computed tomography scan of abdomen with venous contrast demonstrating multiple ill-defined hypoattenuated lesions within the liver and spleen. C) Hematoxylin and eosin stain (original magnification  $\times 200$ ) of a pulmonary lesion revealing prominent eosinophil infiltration of stroma and vessel walls. Arrow indicates a granuloma composed of histiocytes and eosinophils. The prominent eosinophilia was inconsistent with hypersensitivity pneumonitis, and the absence of vessel wall damage did not support a diagnosis of eosinophilic granulomatosis with polyangiitis.

*Echinococcus*, *Fasciola*, and *Schistosoma* antibodies were not detected; concentrated and fixed-stain techniques did not reveal parasites on fecal specimens.

We detected a monoclonal T-cell receptor gene rearrangement, suggesting T-cell driven hypereosinophilic syndrome (HES). Other hematologic and vasculitis investigations were unremarkable. HES treatment began with prednisolone (50 mg/d) and mycophenolate (1 g 2 $\times$ /d). Because of her travel history, possibility of false-negative *Strongyloides* serology, and increased immunosuppression, she received ivermectin (200  $\mu$ g/kg orally) for 2 consecutive days and a repeat dose after 14 days.

A CT scan in mid-2021 showed improvement in the pulmonary and hepatic lesions but unchanged splenic lesions. PBEC was  $0.76 \times 10^9$  in September 2021. We added mepolizumab (interleukin-5

monoclonal antibody, 300 mg every 4 wk) in January 2022 because we were unable to reduce the prednisolone below 20 mg daily without a flare of respiratory symptoms. When PBEC returned within normal range, we tapered the prednisolone dose.

During a 3-month period in 2022, the patient experienced forgetfulness and worsening depression while continuing prednisolone (7.5 mg/d) and mycophenolate and mepolizumab at the same doses. PBEC was within reference range; CRP was 6.4 mg/L. Brain magnetic resonance imaging showed a  $13 \times 10$  mm peripherally enhancing right frontal lobe lesion (Figure 2, panel A). In June 2022, she underwent an open biopsy. We noted a stringlike structure within the lesion, which we removed; it was a live and motile helminth (80 mm long, 1 mm diameter) (Figure 2, panels B, C). We performed a circumferential durotomy and

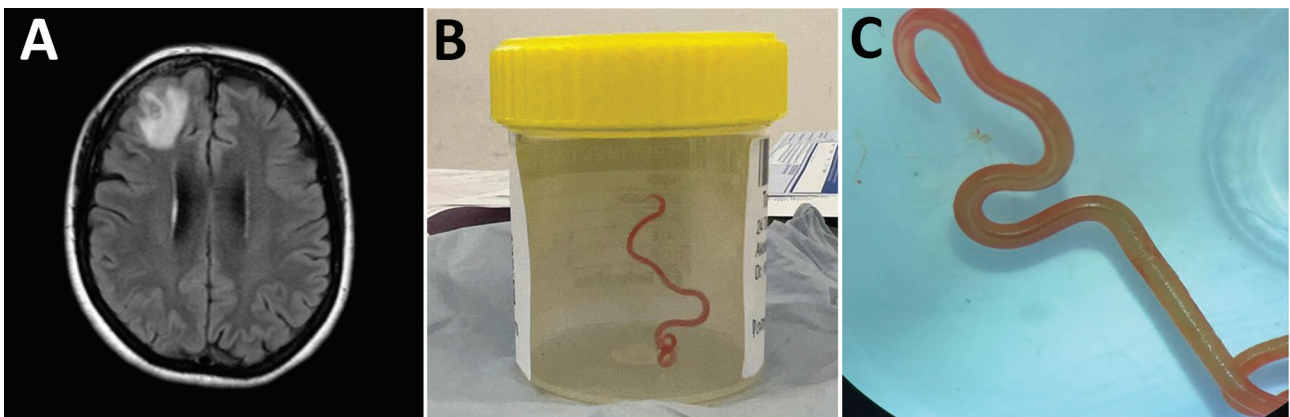


**Figure 2.** Detection of *Ophidascaris robertsi* nematode infection in a 64-year-old woman from southeastern New South Wales, Australia. A) Magnetic resonance image of patient's brain by fluid-attenuated inversion recovery demonstrating an enhancing right frontal lobe lesion,  $13 \times 10$  mm. B) Live third-stage larval form of *Ophidascaris robertsi* (80 mm long, 1 mm diameter) removed from the patient's right frontal lobe. C) Live third-stage larval form of *O. robertsi* (80 mm long, 1 mm diameter) under stereomicroscope (original magnification  $\times 10$ ).

corticotomy and found no other helminths. Histopathology of the dural tissue revealed a benign, organizing inflammatory cavity with prominent eosinophilia.

We provisionally identified the helminth as a third-stage larva of *Ophidascaris robertsi* on the basis of its distinctive red color, 3 active ascaridoid-like lips, presence of a cecum, and absence of a fully developed reproductive system, in the context of the known epidemiologic distribution of this species. The head and tail were preserved at the Australian National Wildlife Collection (W/LHC no. N5758). Small segments underwent independent PCR-based sequencing targeting the cytochrome oxidase c subunit 1 (*cox1*) (5,6) at the University of Sydney and the second internal transcribed spacer (ITS) 2 of nuclear ribosomal DNA (7) at the University of Melbourne. Both sequencing results provided >99.7% sequence match to *Ophidascaris* (formerly *Amplicecum*) *robertsi* isolates in the National Center for Biotechnology Information and in-house databases (Appendix, <https://wwwnc.cdc.gov/EID/article/29/9/23-0351-App1.pdf>).

A progress CT scan revealed resolution of pulmonary and hepatic lesions but unchanged splenic lesions. The patient received 2 days of ivermectin (200 µg/kg/d) and 4 weeks of albendazole (400 mg 2×/d). She was given a weaning course of dexamethasone (starting 4 mg 2×/d) over 10 weeks, while all other immunosuppression was discontinued. Six months after surgery (3 months after ceasing dexamethasone), the patient's PBEC remained normal. Neuropsychiatric symptoms had improved but persisted.

## Conclusions

The patient in this case resided near a lake area inhabited by carpet pythons. Despite no direct snake contact, she often collected native vegetation, warri-gal greens (*Tetragonia tetragonioides*), from around the lake to use in cooking. We hypothesized that she inadvertently consumed *O. robertsi* eggs either directly from the vegetation or indirectly by contamination of her hands or kitchen equipment.

The patient's clinical and radiologic progression suggests a dynamic process of larval migration to multiple organs, accompanied by eosinophilia in blood and tissues, indicative of visceral larva migrans syndrome. We suspect that the splenic lesions are a separate pathology because they remained stable and were not PET avid, unlike the pulmonary and hepatic lesions.

This case highlights the difficulty in obtaining a suitable specimen for parasitic diagnosis and the challenging management decisions regarding im-

munosuppression in the presence of potentially life-threatening HES. Although visceral involvement is common in animal hosts, the invasion of the brain by *Ophidascaris* larvae had not been reported previously. The patient's immunosuppression may have enabled the larvae to migrate into the central nervous system (CNS). The growth of the third-stage larva in the human host is notable, given that previous experimental studies have not demonstrated larval development in domesticated animals, such as sheep, dogs, and cats, and have shown more restricted larval growth in birds and nonnative mammals than in native mammals (4).

After we removed the larva from her brain, the patient received anthelmintics and dexamethasone to address potential larvae in other organs. *Ophidascaris* larvae are known to survive for long periods in animal hosts; for example, laboratory rats have remained infected with third-stage larvae for ≥4 years (4). The rationale for ivermectin and albendazole was based on data from the treatment of nematode infections in snakes and humans (8,9). Albendazole has better penetration into the CNS than ivermectin (10). Dexamethasone has been used in other human nematode and tapeworm infections to avoid deleterious inflammatory CNS responses following treatment (11).

In summary, this case emphasizes the ongoing risk for zoonotic diseases as humans and animals interact closely. Although *O. robertsi* nematodes are endemic to Australia, other *Ophidascaris* species infect snakes elsewhere, indicating that additional human cases may emerge globally.

## Acknowledgments

We thank Mitali Fadia and Sophie Hale for their assistance.

## About the Author

Dr. Hossain is an infectious diseases physician in Australia. Her primary research interest is in parasitology.

## References

1. Sprent JFA. The life history and development of *Amplicecum robertsi*, an ascaridoid nematode of the carpet python (*Morelia spilotes variegatus*). I. Morphology and functional significance of larval stages. *Parasitology*. 1963;53:7-38. <https://doi.org/10.1017/S0031182000072498>
2. Gallego-Agúndez M, Villaluenga Rodríguez JE, Juan-Sallés C, Spratt DM. First report of parasitism by *Ophidascaris robertsi* (Nematoda) in a sugar glider (*Petaurus breviceps*, Marsupialia). *J Zoo Wildl Med*. 2014;45:984-6. <https://doi.org/10.1638/2014-0107.1>
3. Gonzalez-Astudillo V, Knott L, Valenza L, Henning J, Allavena R. Parasitism by *Ophidascaris robertsi* with associated pathology findings in a wild koala

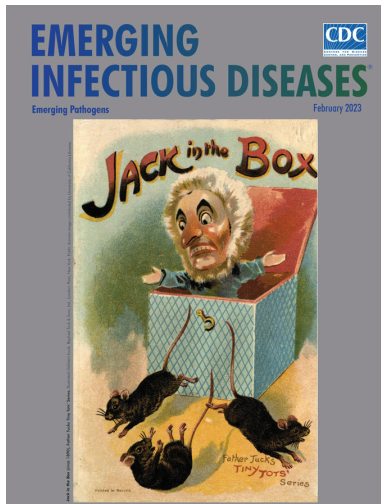
- (*Phascolarctos cinereus*). Vet Rec Case Rep. 2019;7:e000821. <https://doi.org/10.1136/vetreccr-2019-000821>
4. Sprent J. The life history and development of *Amplichaecum robertsi*, an ascaridoid nematode of the carpet python (*Morelia spilotes variegatus*). II. Growth and host specificity of larval stages in relation to the food chain. Parasitology. 1963;53:321–37. <https://doi.org/10.1017/S0031182000072796>
  5. Baron HR, Šlapeta J, Donahoe SL, Doneley R, Phalen DN. Compensatory gastric stretching following subtotal gastric resection due to gastric adenocarcinoma in a diamond python (*Morelia spilota spilota*). Aust Vet J. 2018;96:481–6. <https://doi.org/10.1111/avj.12764>
  6. Folmer O, Black M, Hoeh W, Lutz R, Vrijenhoek R. DNA primers for amplification of mitochondrial cytochrome c oxidase subunit I from diverse metazoan invertebrates. Mol Mar Biol Biotechnol. 1994;3:294–9.
  7. Mullis K, Faloona F, Scharf S, Saiki R, Horn G, Erlich H. Specific enzymatic amplification of DNA in vitro: the polymerase chain reaction. Cold Spring Harb Symp Quant Biol. 1986;51:263–73. <https://doi.org/10.1101/SQB.1986.051.01.032>
  8. Wilson S, Carpenter JW. Endoparasitic diseases of reptiles. J Exot Pet Med. 1996;5:64–74. [https://doi.org/10.1016/S1055-937X\(96\)80019-3](https://doi.org/10.1016/S1055-937X(96)80019-3)
  9. Herman JS, Chioldini PL. Gnathostomiasis, another emerging imported disease. Clin Microbiol Rev. 2009;22:484–92. <https://doi.org/10.1128/CMR.00003-09>
  10. Nau R, Sörgel F, Eiffert H. Penetration of drugs through the blood-cerebrospinal fluid/blood-brain barrier for treatment of central nervous system infections. Clin Microbiol Rev. 2010;23:858–83. <https://doi.org/10.1128/CMR.00007-10>
  11. Katchanov J, Sawanyawisuth K, Chotmongkol V, Nawa Y. Neurognathostomiasis, a neglected parasitosis of the central nervous system. Emerg Infect Dis. 2011;17:1174–80. <https://doi.org/10.3201/eid1707.101433>

Address for correspondence: Sanjaya N. Senanayake, Infectious Diseases Unit, Canberra Health Services, The Canberra Hospital, Yamba Dr, Garran, Australian Capital Territory, Postcode 2605, Australia; email: sanjaya.senanayake@anu.edu.au

February 2023

## Emerging Pathogens

- Infant Botulism, Israel, 2007–2021
- Sentinel Surveillance System Implementation and Evaluation for SARS-CoV-2 Genomic Data, Washington, USA, 2020–2021
- Crimean-Congo Hemorrhagic Fever, Spain, 2013–2021
- *Streptococcus dysgalactiae* Bloodstream Infections, Norway, 1999–2021
- Changing Disease Course of Crimean-Congo Hemorrhagic Fever in Children, Turkey
- Relationship between Telework Experience and Presenteeism during COVID-19 Pandemic, United States, March–November 2020
- Circovirus Hepatitis Infection in Heart-Lung Transplant Patient, France
- Incidence and Transmission Dynamics of *Bordetella pertussis* Infection in Rural and Urban Communities, South Africa, 2016–2018
- Influence of Landscape Patterns on Exposure to Lassa Fever Virus, Guinea
- Increased Multidrug-Resistant *Salmonella enterica* I Serotype 4,[5],12:i:- Infections Associated with Pork, United States, 2009–2018



- Age-Stratified Model to Assess Health Outcomes of COVID-19 Vaccination Strategies, Ghana
- Early Introduction and Community Transmission of SARS-CoV-2 Omicron Variant, New York, New York, USA
- Correlates of Protection, Thresholds of Protection, and Immunobridging among Persons with SARS-CoV-2 Infection
- Longitudinal Analysis of Electronic Health Information to Identify Possible COVID-19 Sequelae
- Nipah Virus Exposure in Domestic and Peridomestic Animals Living in Human Outbreak Sites, Bangladesh, 2013–2015
- (Mis)perception and Use of Unsterile Water in Home Medical Devices, PN View 360+ Survey, United States, August 2021
- Neoehrlichiosis in Symptomatic Immunocompetent Child, South Africa
- Successful Drug-Mediated Host Clearance of *Batrachochytrium salamandrivorans*
- Powassan Virus Lineage I in Field-Collected *Dermacentor variabilis* Ticks, New York, USA
- *Bartonella* spp. and Typhus Group Rickettsiae among Persons Experiencing Homelessness, São Paulo, Brazil
- Novel Prion Strain as Cause of Chronic Wasting Disease in a Moose, Finland
- Novel Species of *Brucella* Causing Human Brucellosis, French Guiana
- Penicillin and Cefotaxime Resistance of Quinolone-Resistant *Neisseria meningitidis* Clonal Complex 4821, Shanghai, China, 1965–2020
- Molecular Detection of *Candidatus Orientia chuto* in Wildlife, Saudi Arabia

**EMERGING  
INFECTIOUS DISEASES**

To revisit the February 2023 issue, go to:  
<https://wwwnc.cdc.gov/eid/articles/issue/29/2/table-of-contents>

# Human Neural Larva Migrans Caused by *Ophidascaris robertsi* Ascarid

## Appendix

### Methods of Identification of the Nematode

At the University of Sydney, a small ( $\approx 3$  mm) central section of the nematode (22P409183; W/LHC# N5758) was resected and used for DNA isolation (Monarch Genomic DNA Purification Kit, NEB, Australia). A fragment ( $\approx 600$  base pair) of the cytochrome oxidase c subunit 1 (*cox1*) was amplified with LCO1490 (5'-GGT CAA CAA ATC ATA AAG ATA TTG G-3') and HCO2198 (5'-TAA ACT TCA GGG TGA CCA AAA AAT CA-3') primers (1). The PCR protocol used MyTaq Red Mix (Bioline) as previously described (2). The PCR product of the expected size was bidirectionally sequenced at MacroGen Inc. (Seoul, South Korea). Sequences were assembled and compared to available nematode sequences in CLC Main Workbench 22 (CLCbio, QIAGEN). Molecular *cox1* identification confirmed that the nematode belonged to the genus *Ophidascaris*. Comparison with our in-house nematode *cox1* sequence barcodes of *Ophidascaris* spp. from Australia, confirmed its close identity (99.7% across the amplified *cox1* region) with a specimen from a carpet python (*Morelia spilota*) located in greater Sydney considered to represent *Ophidascaris robertsi*. The new *Ophidascaris robertsi cox1* sequence is deposited in GenBank under the accession number OP198570. Its phylogenetic relationship to other available *Ophidascaris* species and related ascarid sequences is demonstrated in Appendix Figure 1.

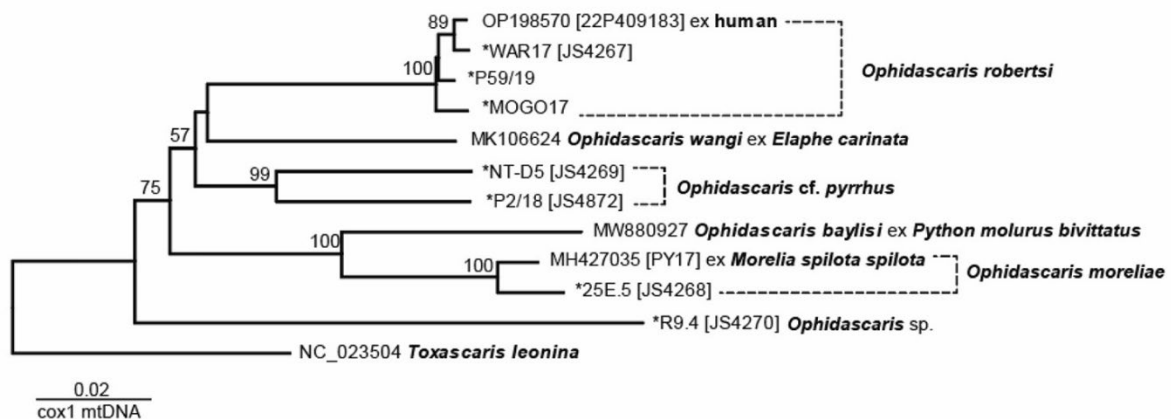
At the University of Melbourne, genomic DNA was extracted from a small portion of the nematode larva by sodium dodecyl-sulfate:proteinase K treatment and purified over a spin column (Wizard Clean-Up, Promega). Subsequently, a region partially spanning the 5.8S and the second internal transcribed spacer of nuclear ribosomal DNA (ITS-2) was amplified from an aliquot of genomic DNA (5–10 ng) by PCR (3) using the oligonucleotide primers NC13: 5'-ATCGATGAAGAACGCAGC-3' (forward) and NC2: 5'-TTAGTTTCTTTTCCTCCGCT-3' (reverse), designed to regions of the 5.8S or 28S ribosomal RNA genes (4). PCR reactions

(50 µL) were performed in 10 mmol Tris–HCl, pH 8.4; 50 mmol KCl; 3.0 mmol MgCl<sub>2</sub>; 250 mmol each of dATP, dCTP, dGTP and dTTP; and 50 pmol of each primer with 1 unit GoTaq polymerase (Promega) under the following conditions: 94°C, 30 s (denaturation); 55°C, 30 s (annealing); 72°C, 30 s (extension) for thirty-five cycles, followed by a final extension at 72°C for five minutes (Thermocycler, Perkin Elmer Cetus). Positive (DNA from *Toxocara canis*; sample Tcan1) and negative (no-DNA) control samples were also included in the amplification run to exclude any ‘carry-over’ contamination. Following thermal cycling, aliquots (2 µL) of the test sample and the positive and negative control samples were examined on 1.5% agarose-TBE (65 mmol Tris–HCl, 27 mmol boric acid, 1 mmol EDTA, pH 9) gel, stained with ethidium bromide, and photographed upon transillumination. An aliquot (5 µL) of the amplicon (i.e., test sample) was treated with ExoSAP-IT (Affymetrix, USA), according to the manufacturer’s instructions, and then subjected to direct, automated sequencing (BigDye Terminator v.3.1 chemistry, Applied Biosystems, USA) in both directions using the same primers (separately) as employed for PCR amplification. The ITS-2 sequence obtained by sequencing from the test sample-amplicon was then subjected to BLASTN analysis (via <https://blast.ncbi.nlm.nih.gov/Blast.cgi>) against all publicly available sequence datasets in the National Centre for Biotechnology Information (NCBI) database. The new *Ophidascaris robertsi* 5.8S to ITS-2 sequence is deposited in GenBank under the accession number OP886196. Its phylogenetic relationship to other available *Ophidascaris* species and related ascarid sequences is demonstrated in Appendix Figure 2.

## References

1. Folmer O, Black M, Hoeh W, Lutz R, Vrijenhoek R. DNA primers for amplification of mitochondrial cytochrome c oxidase subunit I from diverse metazoan invertebrates. *Mol Mar Biol Biotechnol.* 1994;3:294–9. [PubMed](#)
2. Baron HR, Šlapeta J, Donahoe SL, Doneley R, Phalen DN. Compensatory gastric stretching following subtotal gastric resection due to gastric adenocarcinoma in a diamond python (*Morelia spilota spilota*). *Aust Vet J.* 2018;96:481–6. [PubMed](#)  
<https://doi.org/10.1111/avj.12764>
3. Mullis K, Faloona F, Scharf S, Saiki R, Horn G, Erlich H. Specific enzymatic amplification of DNA in vitro: the polymerase chain reaction. *Cold Spring Harb Symp Quant Biol.* 1986;51:263–73. [PubMed](#) <https://doi.org/10.1101/SQB.1986.051.01.032>

4. Chilton NB. The use of nuclear ribosomal DNA markers for the identification of bursate nematodes (order Strongylida) and for the diagnosis of infections. *Anim Health Res Rev.* 2004;5:173–87. [PubMed https://doi.org/10.1079/AHR200497](https://doi.org/10.1079/AHR200497)
5. Katoh K, Standley DM. MAFFT multiple sequence alignment software version 7: improvements in performance and usability. *Mol Biol Evol.* 2013;30:772–80. [PubMed https://doi.org/10.1093/molbev/mst010](https://doi.org/10.1093/molbev/mst010)



**Appendix Figure 1.** Phylogenetic relationship of *Ophidascaris robertsi* *cox1*. The tree was inferred using the minimum-evolution method and evolutionary distances were computed using the maximum composite likelihood method and are in the units of the number of base substitutions per site. The tree is drawn to scale; branch lengths are in the same units as those of the evolutionary distances used to infer the phylogenetic tree. The *cox1* sequence alignment totals 1,470 positions. The percentage (>50%) of replicate trees in which the associated taxa clustered together in the bootstrap test (500 replicates) are shown next to the branches. Evolutionary analyses were conducted in MEGA11 (<https://www.megasoftware.net>). Sequences with \* are unpublished, from a local in-house database at the University of Sydney, Sydney, Australia.



**Appendix Figure 2.** Phylogenetic relationship of *Ophidascaris robertsi* partial 5.8S and ITS-2 region of rRNA. The tree was inferred using the minimum evolution method and evolutionary distances were computed using the maximum composite likelihood method and are in the units of the number of base substitutions per site. The tree is drawn to scale; branch lengths are in the same units as those of the evolutionary distances used to infer the phylogenetic tree. The partial 5.8S and complete ITS-2 region of rRNA sequence alignment totals 592 positions and was aligned using MAFFT (5). The percentage (>50%) of replicate trees in which the associated taxa clustered together in the bootstrap test (2,000 replicates) are shown next to the branches. Evolutionary analyses were conducted in MEGA11 (<https://www.megasoftware.net>).